Chapter 15

Inelastic Scattering of (Anti)neutrinos from Nuclei

15.1 Introduction

We have discussed inelastic processes from free nucleon targets in Chapters 11 and 12. However, most of the early experiments and also the new experiments on inelastic as well as quasielastic reactions induced by (anti)neutrinos use nuclear targets. In this chapter, we will focus on the inelastic process of producing mesons and photons from the nuclear targets. When inelastic processes like

$$\nu_l(\bar{\nu}_l) + N \to l^-(l^+) + N' + m; \;\; N, N' : \text{ proton or neutron and } \; m \; \text{ is a meson,}$$

(discussed in Chapter 12) take place inside a nucleus, the nucleus can stay in the ground state giving almost all the transferred energy in the reaction to the outgoing meson leading to the coherent production of mesons or can be excited and/or broken up leading to the incoherent production of meson. In the subsequent sections, incoherent and coherent pion production from nuclei in the delta dominance model will be discussed with some comments on the inelastic production of kaons and photons.

The first experiments on inelastic scattering of (anti)neutrinos from nuclei were done at CERN in the early 1960s using heavy liquid bubble chambers (HLBC) filled with propane, freon and with spark chambers, and at ANL/BNL with spark and bubble chambers. The importance of nuclear medium effects in the analysis of these experiments was realized and discussed in the context of inelastic as well as quasielastic reactions. Some of the mesons, mostly pions, produced in the inelastic reactions could be absorbed in the parent nucleus giving rise to 'pionless' lepton events in charged current (CC) induced reactions enhancing the yield of quasielastic events and reducing the yield of 'pionic' events as compared to the theoretical predictions for these reactions from free nucleon targets (Chapter 12). While some

https://doi.org/10.1017/9781108489065.016 Published online by Cambridge University Press

theoretical calculations were made to estimate, quantitatively, the effect of nuclear medium effects in quasielastic reactions (see Chapter 14), no serious efforts were made in the case of inelastic reactions. Subsequently, many experiments were done at CERN [696, 697, 698, 699, 700], SKAT [701, 702, 703, 704], FNAL [705, 706], and CHARM [707], using propane, propane– freon, neon, marble, and aluminium targets; only a qualitative description of the nuclear medium effects was used. Most of these experiments studied the incoherent production of pions while some of them also studied the coherent production of pions [698, 699, 700, 703, 704, 706, 708, 709] from nuclei. Later, experiments done with hydrogen and deuterium targets performed at ANL [710, 711], BNL [519], CERN [470, 712, 713], and FNAL [469] were also analyzed without any consideration of deuterium effects. Since most of these experiments were done at very high energies, it was argued that nuclear medium effects may not be important in this energy region.

The theoretical and experimental interest in studying the nuclear medium effects in inelastic reactions induced by (anti)neutrinos on nuclear targets was renewed after the first evidence of neutrino oscillations was reported in the study of atmospheric neutrinos in Kamiokande and IMB experiments (Chapter 18). In these experiments, a deficit in the ratio of muon to electron yield produced in the quasielastic reactions induced by atmospheric (anti)neutrinos $\nu_\mu(\bar{\nu}_\mu)$ and $\nu_e(\bar{\nu}_e)$ when compared to the theoretical predictions was observed and attributed to neutrino oscillations of $\nu_\mu(\bar{\nu}_\mu)$ neutrinos. Since atmospheric (anti)neutrinos have quite a wide spectrum in the range of a few hundreds of MeV to hundreds of GeV, and the spectrum have higher flux at lower energies, the inelastic production of pions plays a very important role in the total event rates. A knowledge of the nuclear medium effects in the inelastic production of pions is important in the analysis of these experiments for the following reasons.

i) While identifying the quasielastic lepton events, the 'pionless' lepton events (now called the 'quasielastic like' events) discussed earlier, in the context of neutrino experiments at CERN, contribute to a major source of uncertainty in the systematics as they may overlap in energy with genuine quasielastic events due to the momentum distribution of nucleons in the nucleus. Theoretically, it is quite difficult to estimate quasielastic-like events, as it requires the knowledge of reaction mechanisms for inelastic pion production from the nucleon in the presence of nuclear medium effects as well as a mechanism for pion absorption in the nuclear medium.

ii) The charged pions $\pi^-(\pi^+)$ produced in the inelastic (anti)neutrino reactions constitute a major source to the background in identifying the genuine lepton events produced by the quasielastic reactions. This is because the charged pions produced by neutral currents (NC) in nuclei through various channels described in Chapter 12, could be misidentified with charged muons $\mu^-(\mu^+)$ in the IMB and Kamiokande detectors; these detectors use Cerenkov radiation. Even in the case of charged current (CC) induced reactions (Chapter 12), when the muon is produced with high energy and the pion is produced with low energy, the muons may escape the detector, while the pions may be misidentified as muons. This is likely to happen in the case of (anti)neutrino beams with a continuous energy spectrum of (anti)neutrinos spanning a wide energy range between $0.3 < E_{\nu(\bar{\nu})} < 3$ GeV.

https://doi.org/10.1017/9781108489065.016 Published online by Cambridge University Press

iii) In the case of $\nu_e(\bar{\nu}_e)$ neutral current (NC) induced π^0 production, these pions would promptly decay into photons $(\pi^0 \rightarrow 2\gamma)$ giving electrons and positrons through pair creation $(\gamma \rightarrow e^+e^-)$. Some of these electrons (positrons) which do not escape the detector, will produce Bremsstrahlung photon signals in the detector which would mimic genuine quasielastic electron (positron) events produced by the atmospheric (anti)neutrinos.

In the aforementioned scenario, the inelastic production of pions both in the CC and NC channels contribute a major source of background in most of the present neutrino oscillation experiments.

It was therefore emphasized that the neutrino event generators NUANCE [535] and NEUT [714, 607] incorporating earlier calculations of Rein and Sehgal [492, 715] for incoherent and coherent pion production should be modified to include the nuclear medium effects. The only consideration of the nuclear medium effects included in these analyses was from the works of Smith and Moniz in the non-relativistic global Fermi gas model [657]. The other major source of nuclear medium effects in the inelastic production of pions are the well-known effects due to the final state interactions of pions with the residual nucleus. This type of nuclear medium effects are reasonably well modeled in the neutrino event generators like NUANCE [535] and NEUT [714, 607] based on the Valencia model (for discussion see Ref. [356]). These neutrino event generators were used to analyze the neutrino oscillation experiments of IMB and Kamiokande collaborations.

In view of these developments in neutrino oscillation physics and the earlier results of the LSND neutrino experiment[716] indicating the possibility of the existence of a fourth flavor, that is, sterile neutrino, new experiments like K2K, SciBooNE, MiniBooNE, T2K, NOvA, ArgoNeuT, MINERvA, etc. were planned and done in the energy region of $\sim$ 1 GeV, using detectors with moderate nuclear targets like ^{12}C, ^{16}O, etc.(for details see Chapter 17) which measured the neutrino–nucleus cross sections for the quasielastic and inelastic production of pions.

The importance of the nuclear medium effects in the inelastic pion production in analyzing neutrino oscillation experiments was emphasized quite early by Kim et al.[717] and Singh et al. [718], in the case of incoherent production of pions and by Kim et al. [719] and Kelkar et al. [720] in the case of coherent pion production. Subsequently, many microscopic calculations employing sophisticated nuclear wave functions as well as models like relativistic Fermi gas, relativistic mean field and other approximation methods were performed to estimate the nuclear medium effects. Many of them included contributions from MEC and other correlation effects beyond impulse approximation. The details of the various methods are given in Refs. [721, 722, 723, 482, 724, 664, 725, 726, 483, 727, 668, 692, 728, 729, 730, 731, 732, 733]. For a historical development, readers are referred to excellent reviews [426, 356, 678, 731] on the subject.

In case of deuterium experiments, the early theoretical calculations for the (anti)neutrino induced disintegration of deuterons were done without nuclear medium effects, using perturbation theory in impulse approximation with sophisticated two-nucleon wave functions for the deuteron. Recently, elaborate calculations using coupled channel methods and T matrix

https://doi.org/10.1017/9781108489065.016 Published online by Cambridge University Press

expansion have been done showing large effects due to the final state interactions in some channels [734]. Therefore, there are two types of nuclear medium effects which are present both in the incoherent and coherent production of pions from nuclei, that is, in the production process and the final state interactions. We would describe them briefly in this chapter.

The experimental study of incoherent pion production has been recently made at K2K [735, 736], MiniBooNE [737, 738], SciBooNE [739], NOMAD [740], ArgoNeuT [741], MINERvA [742, 743, 744], T2K [745], etc. collaborations, mostly in the energy region of a few hundreds of MeV to a few GeV. Recent experimental study to measure coherent pion production cross section in this energy region has been made by K2K [746], MiniBooNE [747], SciBooNE [748, 749], NOMAD [740], ArgoNeuT [750], MINERvA [751], T2K [752], etc. collaborations.

In this chapter, we will describe some of the effects described here and their effects on the analysis of current neutrino oscillation experiments. We also briefly describe the nuclear medium effects in some other inelastic processes like the reactions in which (anti)kaons or photons are emitted in charged (neutral) current induced reactions like

$$\nu_\mu(\nu_e) + {}^A_Z X \rightarrow \mu^-(e^-) + {}^A_{Z+1}X, \tag{15.1}$$

$$\nu_\mu(\bar{\nu}_\mu) + {}^A_Z X \rightarrow \nu_\mu(\bar{\nu}_\mu) + {}^A_Z X + \gamma, \tag{15.2}$$

and reactions in which hyperons are produced, that is, $\bar{\nu}_l + {}^A_Z X \rightarrow l^+ + {}^A_\Lambda Y$. The hyperon produced in the final state is identified by its decay into pions and nucleons which is also affected by the nuclear medium effects.

15.2 Charged Current Inelastic Reactions

15.2.1 Incoherent meson production

The early experiments done on inelastic pion production emphasized the need for including nuclear medium effects but these effects were not used in the analyses of the experiments. The calculations for the final state interaction of pions in neutrino induced pion production were done by Adler et al. [753]. In recent years, these effects have been taken into account by many authors. The nuclear medium effects in the production process have been mostly calculated in the Fermi gas model [721, 722, 723, 482, 724, 664, 725, 726, 483, 727, 668, 692] with some calculations made using relativistic spectral function and relativistic plane wave approximation (RPWA) with nuclear wave functions [722, 728, 729, 730, 731, 732, 733]. The final state interactions have been calculated in various approaches and some are discussed in Section 15.4.2.

In this section, we discuss the inelastic charged current lepton production accompanied by a meson(Figure 15.1) in the relativistic Fermi gas model using local density approximation. To take into account the Fermi motion and Pauli blocking effect in the local density approximation (LDA) (Chapter 14), first a general expression for the differential scattering cross section is obtained.

https://doi.org/10.1017/9781108489065.016 Published online by Cambridge University Press

The differential scattering cross section for (anti)neutrinos interacting with a bound nucleon and producing a meson m, inside a nucleus, $\nu_l(k) + N(p) \rightarrow l^-(k') + N'(p') + m(p_m)$, in LDA is written as [754]:

$$\left(\frac{d\sigma}{dE_m d\Omega_m}\right)_{\nu A} = \int d^3r\, \rho_n(r) \left(\frac{d\sigma}{dE_m d\Omega_m}\right)_{\nu N}, \tag{15.3}$$

where $\left(\frac{d\sigma}{dE_m d\Omega_m}\right)_{\nu N}$ is the free (anti)neutrino–nucleon differential scattering cross section discussed in Chapter 12, with the condition that the energy of the initial nucleon $E_N < E_F^N(r)$ and the final nucleon $E_{N'}(= E_N + q_0 - E_m) > E_F^{N'}(r)$, at the production point r.

In a symmetric nuclear matter, the differential scattering cross section is written as

$$\left(\frac{d\sigma}{dE_m d\Omega_m}\right)_{\nu A} = 2\int d^3r \sum_{N=n,p} \int \frac{d^3p_N}{(2m)^3}\, \Theta(E_F^N(r) - E_N)\Theta(E_N + q_0 - E_m - E_F^{N'}(r)) \left(\frac{d\sigma}{dE_m d\Omega_m}\right)_{\nu N},$$

where $E_N = \sqrt{|\vec{p}_N|^2 + M^2}$; $\vec{k} + \vec{p}_N = \vec{k}' + \vec{p}'_N + \vec{p}_m$.

Using energy–momentum conservation, $E_{N'}$ may be written as

$E_{N'} = \sqrt{|\vec{P}|^2 + |\vec{p}_N|^2 + 2|\vec{P}||\vec{p}_N| cos\theta_N + M^2}$, where $\vec{P} = \vec{q} - \vec{p}_m$ and $\vec{q} = \vec{k} - \vec{k}'$.

This results in

$$\begin{aligned}\left(\frac{d\sigma}{dE_m d\Omega_m}\right)_A &= 2\int_0^\infty 4\pi r^2 dr \int_\in^{E_F^N(r)} dE_N \int_0^{2\pi} d\phi_N \int_{-1}^{+1} d\cos\theta_N \frac{|\vec{p}_N| E_N}{(2\pi)^3} \\ &\times \Theta(E_F^N(r) - E_N)\, \Theta(E_N + q_0 - E_m - E_F^{N'}(r)) \\ &\times \frac{G_F^2 cos^2\theta_c}{8M_N E_\nu} \frac{|\vec{p}_l||\vec{p}_m|}{E'_N} \frac{1}{(2\pi)^5} \delta^0(q_0 + E_N - E_F^{N'}(r) - E_m) \\ &\times L^{\mu\nu} J_{\mu\nu}\; dE_l d\Omega_l. \end{aligned} \tag{15.4}$$

In this expression, $L^{\mu\nu} = \sum\overline{\sum} l^\mu {l^\nu}^\dagger$ and $J_{\mu\nu} = \sum\overline{\sum} j_\mu {j_\nu}^\dagger$, where l^μ is the leptonic current and j_μ is the hadronic current; both are given in Chapter 12. Furthermore, the azimuthal angle dependence have been found to be very small for pion production in electron and photon induced processes; the integration over the azimuthal angle can be replaced by 2π [754].

The delta integration in Eq. (15.4) is performed using energy conservation

$$q_0 + \sqrt{|\vec{p}_N|^2 + M^2} - \sqrt{|\vec{P}|^2 + |\vec{p}_N|^2 + 2|\vec{P}||\vec{p}_N| cos\theta_N + M^2} - E_m = 0,$$

which on simplifying gives

$$\cos\theta_N = \frac{P^2 + 2E_N P_0}{2|\vec{P}||\vec{p}_N|};\;\; P_0 = q_0 - E_m,\;\; \frac{P^2 + 2E_N P_0}{2|\vec{P}||\vec{p}_N|} \leq 1 \;\text{ as }\; abs(\cos\theta_N) \leq 1,$$

and

$$E_N^2 + E_N P_0 + \frac{P^2}{4} + \frac{M^2|\vec{P}|^2}{P^2} \leq 0,$$

https://doi.org/10.1017/9781108489065.016 Published online by Cambridge University Press

which results in

$$\in' = \frac{-P_0 + \sqrt{P_0^2 - 4\left(\frac{P^2}{4} + \frac{M^2|\vec{P}|^2}{P^2}\right)}}{2}.$$

Thus, the lower limit in Eq. (15.4), for $\in$ is constrained to

$$\in = max(M, E_F^{N'} - P_0, \in').$$

The final expression to evaluate the differential scattering cross section is approximated as

$$\begin{aligned}\left(\frac{d\sigma}{dE_m d\Omega_m}\right)_A &= \frac{G_F^2 cos^2\theta_c}{64\pi^5}\int_0^\infty r^2 dr \int dE_N dE_l d\Omega_l \frac{|\vec{p}_l||\vec{p}_m|}{|\vec{P}||\vec{k}|}(E_F^N(r) - \epsilon) \\ &\times \Theta(E_F^N(r) - \in)\Theta(-P^2)\Theta(P_0)L^{\mu\nu}J_{\mu\nu}(|\vec{p}_{N'}|, q, k_m) \\ &\times \left(\frac{d\sigma}{dE_m dcos\theta_m}\right)_N,\end{aligned}$$

where

$$|\vec{p}_{N'}| = \sqrt{E_{N'}^2 - M^2} \text{ and } E_{N'} = \frac{E_F^N(r) + \in}{2}.$$

This prescription is valid for any meson production, where the initial nucleon is below the Fermi sea and the final nucleon is above the Fermi sea. Moreover, the nucleus is at rest and not the nucleons.

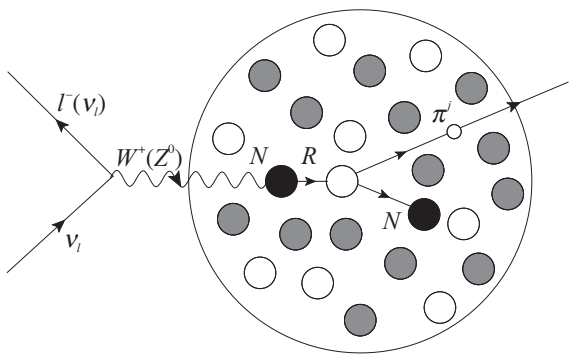

Figure 15.1 In a neutrino induced reaction on a nucleon target, when a pion is produced in the nuclear medium and comes out without FSI (final state interaction). The open (shaded circles represent protons (neutrons) inside a nucleus and the dark shaded circle represents a nucleon (p or n) with which a neutrino interacts through a CC (NC) reaction and a non-resonant or a resonant state (R) is formed, which gives rise to a p or n and a pion (π^i), where i represents the charge state. For example, in a CC reaction $\nu_l + n \to l^- + R^+$, R^+ may give a p and π^0 or a n and π^+; then the pion comes out without FSI with the residual nucleus.

The nuclear medium effects in single pion production has been widely studied; moreover, the present generation of neutrino experiments frequently analyze these events. Therefore,

https://doi.org/10.1017/9781108489065.016 Published online by Cambridge University Press

in the next section, we describe the nuclear medium effects in incoherent one-pion production processes. Moreover, we have seen in Chapter 12, that the pion production is mainly dominated by the formation of delta as the resonant state and its subsequent decay. Therefore, the present discussion is confined to medium modification of the delta properties.

15.2.2 Pion production in the delta dominance model

In an inelastic reaction where a Δ is produced in the intermediate state and subsequently decays to a nucleon and a pion, the various possible channels for a pion production in the (anti)neutrino interactions on a nucleon target are

$$\begin{aligned} \nu_l(k) + p(p) \;\; &\rightarrow \;\; l^-(k') + \Delta^{++}(p') \\ &\qquad\quad \searrow p + \pi^+ \end{aligned} \qquad\qquad \begin{aligned} \nu_l(k) + n(p) \rightarrow l^-(k') + \Delta^{+}(p') \\ \searrow p + \pi^0 \\ \searrow n + \pi^+ \end{aligned} \tag{15.5}$$

$$\begin{aligned} \bar{\nu}_l(k) + n(p) \;\; &\rightarrow \;\; l^+(k') + \Delta^{-}(p') \\ &\qquad\quad \searrow n + \pi^- \end{aligned} \qquad\qquad \begin{aligned} \bar{\nu}_l(k) + p(p) \rightarrow l^+(k') + \Delta^{0}(p') \\ \searrow p + \pi^- \\ \searrow n + \pi^0 \end{aligned} \tag{15.6}$$

The differential cross section for the reaction $\nu(k) + p(p) \rightarrow \mu^-(k') + \Delta^{++}(p_\Delta)$ can be written as

$$d\sigma = \frac{(2\pi)^4 \delta^4(k + p - p_\Delta - k')}{4ME_\nu} \frac{d\vec{k}'}{(2\pi)^3 2E_{k'}} \frac{d\vec{p}_\Delta}{(2\pi)^3 2E_\Delta} \overline{\sum} \sum |\mathcal{M}|^2. \tag{15.7}$$

Using the following relation,

$$d\vec{k}' = |\vec{k}'|^2 \, d|\vec{k}'| \, d\Omega_{k'} \;=\; E_{k'} \, |\vec{k}'| \, dE_{k'} \, d\Omega_{k'}, \tag{15.8}$$

we get after integrating over Δ momentum,

$$\frac{d\sigma}{dE_{k'} d\Omega_{k'}} = \frac{1}{16\pi^2} \frac{1}{4ME_\nu} |\vec{k}'| \, \frac{1}{E_\Delta} \, \delta(E_p + q_0 - E_\Delta) \, \overline{\sum} \sum |\mathcal{M}|^2. \tag{15.9}$$

To take into account the decay width of Δ, we replace

$$\delta(E_p + q_0 + E_\Delta) \longrightarrow -\frac{1}{\pi} \mathrm{Im} \left[\frac{1}{E_p + q_0 - E_\Delta + i\Gamma/2} \right], \tag{15.10}$$

where the relation

$$\frac{1}{x - x_0 \mp i\epsilon} = P \frac{1}{x - x_0} \pm i\pi\delta(x - x_0) \tag{15.11}$$

https://doi.org/10.1017/9781108489065.016 Published online by Cambridge University Press

is used.

Moreover, one may write

$$\frac{M_\Delta}{E_\Delta}\,\delta(p_\Delta^0 - E_\Delta) \to -\frac{1}{\pi}\,\mathrm{Im}\left[\frac{1}{W - M_\Delta + i\frac{1}{2}\Gamma(W)}\right] \to \frac{1}{\pi}\left[\frac{\frac{\Gamma(W)}{2}}{(W-M_\Delta)^2 + \frac{\Gamma^2(W)}{4}}\right] \quad (15.12)$$

using

$$\delta(W - M_\Delta) = \frac{1}{p_\Delta^0/W}\delta(p_\Delta^0 - E_\Delta) \simeq \frac{M_\Delta}{E_\Delta}\delta(p_\Delta^0 - E_\Delta) \quad (15.13)$$

where $W = \sqrt{p'^2} = \sqrt{{p_\Delta^0}^2 - \vec{p}_\Delta^2}$ is the invariant mass of Δ and $\Gamma(W)$ is the rest width of Δ.

Using Eq. (15.13), Eq. (15.7) is obtained as

$$\frac{d\sigma}{dE_{k'}d\Omega_{k'}} = \frac{1}{16\pi^3}\,\frac{1}{4ME_\nu}\,\frac{|\vec{k}'|}{M_\Delta}\left[\frac{1}{W - M_\Delta + i\frac{1}{2}\Gamma(W)}\right]\overline{\sum}\sum|\mathcal{M}|^2. \quad (15.14)$$

The expression of Q^2-distribution is obtained as

$$\frac{d\sigma}{dQ^2} = \frac{\pi}{E_\nu E_{k'}}\,\frac{d\sigma}{d\Omega_{k'}} \quad (15.15)$$

using which, we may write

$$\frac{d\sigma}{dE_{k'}dQ^2} = \frac{1}{64\pi^2}\,\frac{1}{M^2E_\nu^2}\,\frac{M}{M_\Delta}\,\frac{|\vec{k}'|}{E_{k'}}\left[\frac{\Gamma(W)}{(W-M_\Delta)^2 + \frac{\Gamma^2(W)}{4}}\right]\overline{\sum}\sum|\mathcal{M}|^2. \quad (15.16)$$

Finally, neglecting lepton mass so that $|\vec{k}'|\,d|\vec{k}'| = E_{k'}\,dE_{k'}$ and integrating over lepton energy, we get

$$\frac{d\sigma}{dQ^2} = \frac{G^2\cos^2\theta_C}{128\pi^2}\,\frac{1}{M^2E_\nu^2}\,\frac{M}{M_\Delta}\int_{E_{k'}^{\min}}^{E_{k'}^{\max}} dE_{k'}\,L_{\mu\nu}J^{\mu\nu}\left[\frac{\Gamma(W)}{(W-M_\Delta)^2 + \frac{\Gamma^2(W)}{4}}\right]. \quad (15.17)$$

When a neutrino interacts with a bound nucleon, the nucleon inside the nucleus is constrained to have a momentum below the Fermi momentum, while there is no such constraint on the momentum of the intermediate Δ produced in the medium. The Δ propagates in the medium and experiences all kinds of self energy (Σ_Δ) interactions. This self energy is assumed to be the function of the nuclear density $\rho(\vec{r})$. It involves the decay of Δ-isobar through $\Delta \to N\pi$ channel in the nucleus. However, their decay, is influenced by the Pauli blocking. The nucleons produced in these decay processes have to be above the Fermi momentum $k_F(r)$ of the nucleons in the nucleus thus inhibiting the decay as compared to the free decay of the Δ-isobar described by Γ in Eq. (15.13). This leads to a modification in the decay width of the Δ resonance which has been studied by many authors [755, 756, 757, 758, 759]. Further, there are additional

https://doi.org/10.1017/9781108489065.016 Published online by Cambridge University Press

decay channels open for the Δ resonance in the nuclear medium. In the nuclear medium, the Δ resonance decays through two- and three-body absorption processes like $\Delta N \rightarrow NN$ and $\Delta NN \rightarrow NNN$ through which Δ disappear in the nuclear medium without producing a pion, while a two-body Δ absorption process like $\Delta N \rightarrow \pi NN$ gives rise to some more pions. These nuclear medium effects on the Δ propagation are included by describing the modified mass and the decay width in terms of the Δ self energy used by the parameterization of Oset and Salcedo [755]. The real part of the delta self energy contributes to the mass of Δ and the imaginary part of the delta self energy contributes to the decay width of Δ. These modifications are parameterized by making density dependent changes in mass and decay width in a local density approximation, to the Δ-hole model.

The modification of the mass and width arises from the following sources:
(a) The intermediate nucleon state is partly blocked for the Δ decay because some of these states are occupied (Pauli blocking). The decayed nucleon must be in an unoccupied state. The Pauli correction is taken into account by assuming a local Fermi sea at each point of the nucleus of density $\rho(\vec{r})$, and forcing the nucleon to be above the Fermi sea. This leads to an energy dependent modification in the Δ decay width given as [755]

$$\Gamma \rightarrow \tilde{\Gamma} - 2\mathrm{Im}\Sigma_{\Delta}, \tag{15.18}$$

where $\tilde{\Gamma}$ is the Pauli blocked width of Δ in the nuclear medium and Σ_{Δ} is the self energy of Δ in the nuclear medium and its relativistic form is

$$\tilde{\Gamma} = \frac{1}{6\pi}\left(\frac{f_{\pi N\Delta}}{m_{\pi}}\right)^2 \frac{M}{\sqrt{s}} |\vec{p}\,'_{\mathrm{cm}}|^3 \, F(k_F, E_{\Delta}, p_{\Delta}), \tag{15.19}$$

where

$$|\vec{p}\,'_{\mathrm{cm}}| = \frac{\sqrt{(s - M^2 - m_{\pi}^2)^2 - 4M^2 m_{\pi}^2}}{2\sqrt{s}}, \tag{15.20}$$

and $F(k_F, E_{\Delta}, p_{\Delta})$, the Pauli correction factor is written as [755, 760]

$$F(k_F, E_{\Delta}, p_{\Delta}) = \frac{p_{\Delta}|\vec{p}\,'_{\mathrm{cm}}| + E_{\Delta}E'_{p_{\mathrm{cm}}} - E_F\sqrt{s}}{2p_{\Delta}|\vec{p}\,'_{\mathrm{cm}}|} \tag{15.21}$$

where k_F is the Fermi momentum, $E_F = \sqrt{M^2 + k_F^2}$ and $\vec{p}\,'_{\mathrm{cm}}$, $E'_{p_{\mathrm{cm}}}$ are the nucleon momentum and the relativistic nucleon energy in the final πN center of mass frame.

If $F(k_F, E_{\Delta}, p_{\Delta}) > 1$, it is replaced by 1. Similarly, if $F(k_F, E_{\Delta}, p_{\Delta}) < 0$, then it is replaced by 0 in Eq. (15.19).

https://doi.org/10.1017/9781108489065.016 Published online by Cambridge University Press

In the aforementioned expression, $\sqrt{s}$ is the center of mass energy in the Δ rest frame averaged over the Fermi sea, $\bar{s}$ and is given as

$$\bar{s} = M^2 + m_\pi^2 + 2E_\pi \left(M + \frac{3}{5}\frac{k_F^2}{2M} \right). \tag{15.22}$$

(b) The produced nucleon in the Δ decay inside the nuclear medium feels a single particle potential due to all the other nucleons in the nucleus, known as the binding effect, which is taken care of by the real part of the Δ self energy. This effect modifies the mass of Δ in the medium as

$$M_\Delta \rightarrow \tilde{M}_\Delta = M_\Delta + \mathrm{Re}\Sigma_\Delta. \tag{15.23}$$

The Δ self energy plays a very important role in the different pion nuclear reactions. A thorough study of the Δ self energy is made, using the explicit model by Oset and Salcedo [755]. For the scalar part of the Δ self energy, the numerical results are parameterized in the approximate analytical form (excluding the Pauli corrected width), and are given as [755, 760]:

$$-\mathrm{Im}\Sigma_\Delta = C_Q \left(\frac{\rho}{\rho_0}\right)^\alpha + C_{A2}\left(\frac{\rho}{\rho_0}\right)^\beta + C_{A3}\left(\frac{\rho}{\rho_0}\right)^\gamma, \tag{15.24}$$

which is determined mainly by the one-pion interactions in the nuclear medium. This includes the two-body, three-body, and the quasielastic absorption contributions for the produced pions in the nucleus. The coefficients C_Q accounts for the quasielastic part, the term with C_{A2} for two-body absorption and the one with C_{A3} for three-body absorption, and are parameterized in the range of energies 80 MeV$< T_\pi <$320 MeV, where T_π is the pion kinetic energy, as [755, 760]:

$$C(x) = ax^2 + bx + c, \qquad x = \frac{T_\pi}{m_\pi} \tag{15.25}$$

where C stands for all the coefficients, that is, C_Q, C_{A2}, C_{A3}, α, and $\beta(\gamma = 2\beta)$. The different coefficients used here are tabulated in Table 15.1 and Table 15.2 [755].

Table 15.1 Coefficients used in Eq. (15.24) for the calculation of $\mathrm{Im}\Sigma_\Delta$ as a function of energy in the case of pion nuclear scattering.

T_π(MeV)	C_Q(MeV)	C_{A2}(MeV)	C_{A3}(MeV)	α	β	γ
85	9.7	18.9	3.7	0.79	0.72	1.44
125	11.9	17.7	8.6	0.62	0.77	1.54
165	12.0	16.3	15.8	0.42	0.80	1.60
205	13.0	15.2	18.0	0.31	0.83	1.66
245	14.3	14.1	20.2	0.36	0.85	1.70
315	9.8	13.1	14.7	0.42	0.88	1.76

https://doi.org/10.1017/9781108489065.016 Published online by Cambridge University Press

Table 15.2 Coefficients used for an analytical interpolation of $C(T_\pi)$ of Eq. (15.25).

	C_Q(MeV)	C_{A2}(MeV)	C_{A3}(MeV)	α	β
a	–5.19	1.06	–13.46	0.382	–0.038
b	15.35	–6.64	46.17	–1.322	0.204
c	2.06	22.66	–20.34	1.466	0.613

The real part of the Δ self energy [760] is approximately given by

$$\mathrm{Re}\Sigma_\Delta \simeq 40.0 \left(\frac{\rho}{\rho_0}\right) \mathrm{MeV}. \tag{15.26}$$

These considerations lead to the following modifications in the width $\tilde{\Gamma}$ and mass M_Δ of the Δ resonance:

$$\frac{\Gamma}{2} \to \frac{\tilde{\Gamma}}{2} - \mathrm{Im}\Sigma_\Delta \ \text{ and } \ M_\Delta \to \tilde{M}_\Delta = M_\Delta + \mathrm{Re}\Sigma_\Delta. \tag{15.27}$$

With these modifications, the differential scattering cross section may be written as

$$\frac{d^2\sigma}{dE_{k'}d\Omega_{k'}} = \frac{1}{64\pi^3}\int d\vec{r}\rho_p(\vec{r})\frac{|\vec{k}'|}{E_k}\frac{1}{MM_\Delta}\frac{\frac{\tilde{\Gamma}}{2} - \mathrm{Im}\Sigma_\Delta}{(W-\tilde{M}_\Delta)^2 + (\frac{\tilde{\Gamma}}{2} - \mathrm{Im}\Sigma_\Delta)^2}\overline{\sum}\sum|\mathcal{M}|^2. \tag{15.28}$$

For the lepton production from neutron targets, $\rho_p(\vec{r})$ in this expression is replaced by $\frac{1}{3}\rho_n(\vec{r})$. Therefore, the total scattering cross section for the neutrino induced lepton production process for incoherent 1π production in the nucleus is given by

$$\sigma = \frac{1}{64\pi^3}\iint d\vec{r}\frac{d\vec{k}'}{E_kE_{k'}}\frac{1}{MM_\Delta}\frac{\frac{\tilde{\Gamma}}{2} - \mathrm{Im}\Sigma_\Delta}{(W-\tilde{M}_\Delta)^2 + (\frac{\tilde{\Gamma}}{2.} - \mathrm{Im}\Sigma_\Delta)^2}\left[\rho_p(\vec{r}) + \frac{1}{3}\rho_n(\vec{r})\right]\overline{\sum}\sum|\mathcal{M}|^2. \tag{15.29}$$

It should be noted that $\tilde{\Gamma}$ describes the Δ decaying into nucleons and pions. The various terms in the $\mathrm{Im}\Sigma_\Delta$ correspond to the different responses of Δ in the nuclear medium as explained earlier. The C_Q term in $\mathrm{Im}\Sigma_\Delta$ gives additional contribution to the pion production which arises solely due to nuclear medium effects. Some of the Δs are absorbed through two-body and three-body absorption processes and do not lead to pion production. These are described by C_{A2} and C_{A3} terms in the expression for $\mathrm{Im}\Sigma_\Delta$ given in Eq. (15.24) and do not contribute to the lepton production accompanied by pions. These constitute quasielastic-like events besides the pions which are physically produced but reabsorbed in the nucleus due to FSI; this will be discussed later in the text. Only the C_Q term in the expression for $\mathrm{Im}\Sigma_\Delta$(Eq. (15.24)) contributes to the lepton production accompanied by a pion.

For example, in the case of the one π^+ production process, $\tilde{\Gamma}$ and the C_Q term in $\mathrm{Im}\Sigma_\Delta$ contribute to the pion production. Further, for neutrinos giving rise to π^+ after the interaction with a nucleon target, if the nucleon happens to be a proton, then all the interactions with

https://doi.org/10.1017/9781108489065.016 Published online by Cambridge University Press

protons will give rise to π^+; but if the nucleon is a neutron target ($\nu_l + n \rightarrow l^- + \Delta^+$), then it may give rise to a π^+ or a π^0 which in the absence of FSI may be directly obtained using Clebsch–Gordan coefficients. Therefore, for a charged current, one π^+ production on the neutron target, $\frac{1}{3}\rho_n(\vec{r})$ in the aforementioned expression is replaced by $\frac{1}{9}\rho_n(\vec{r})$. Thus, the total scattering cross section for the neutrino induced charged current one π^+ production on a nucleon target is given by

$$\sigma = \frac{1}{64\pi^3}\int\int d\vec{r}\frac{d\vec{k}'}{E_k E_{k'}}\frac{1}{MM_\Delta}\left[\frac{\frac{\tilde{\Gamma}}{2} - C_Q\left(\frac{\rho}{\rho_0}\right)^\alpha}{(W - M_\Delta - \mathrm{Re}\Sigma_\Delta)^2 + (\frac{\tilde{\Gamma}}{2} - \mathrm{Im}\Sigma_\Delta)^2}\right]\left[a\rho_p(\vec{r}) + b\rho_n(\vec{r})\right]\overline{\sum}\sum|\mathcal{M}|^2 \tag{15.30}$$

Similarly, for an antineutrino reaction, the role of $\rho_p(\vec{r})$ and $\rho_n(\vec{r})$ are interchanged; thus, $\left[a\rho_p(\vec{r}) + b\rho_n(\vec{r})\right]$ in this expression is replaced by $\left[a\rho_n(\vec{r}) + b\rho_p(\vec{r})\right]$ and the antisymmetric term in the leptonic tensor $L_{\mu\nu}$ changes sign , where $a = 1$ and $b = \frac{1}{9}$ for $\pi^+(\pi^-)$ production and $a = 0$ and $b = \frac{2}{9}$ for π^0 production.

15.2.3 Quasielastic-like production of leptons

In a nuclear medium, when a neutrino interacts with a nucleon inside the nucleus, the Δ which is formed may disappear through two- and three-body absorption processes like $\Delta N \rightarrow NN$ and $\Delta NN \rightarrow NNN$ and thus, mimic the quasielastic reaction discussed in the previous section. These Δ absorption processes are described by the C_{A2} and C_{A3} terms in the expression of $\mathrm{Im}\Sigma_\Delta$ given in Eq. (15.24). To estimate the number of quasielastic-like lepton events (without a pion), we write the expression for the total scattering cross section as

$$\sigma = \frac{1}{64\pi^3}\int\int d\vec{r}\frac{d\vec{k}'}{E_k E_{k'}}\frac{1}{MM_\Delta}\frac{C_{A2}\left(\frac{\rho}{\rho_0}\right)^\beta + C_{A3}\left(\frac{\rho}{\rho_0}\right)^\gamma}{(W - M_\Delta - \mathrm{Re}\Sigma_\Delta)^2 + (\frac{\tilde{\Gamma}}{2} - \mathrm{Im}\Sigma_\Delta)^2}\left[\rho_p(\vec{r}) + \frac{1}{3}\rho_n(\vec{r})\right]\overline{\sum}\sum|\mathcal{M}|^2 \tag{15.31}$$

β and γ are tabulated in Table 15.2.

15.3 Coherent Pion Production

15.3.1 Introduction

Coherent pion production has been observed experimentally at higher energies in several nuclei [703, 700, 708, 705, 706, 709] and was studied theoretically using models based on PCAC. The only nuclear medium effect considered in these calculations is the distortion of the final pion. In the CC coherent pion production induced by neutrinos ($\nu + A \rightarrow A + \mu^- + \pi^+$), the nucleus remains in its ground state. The process consists of a weak pion production followed by the strong distortion of the pion in its way out of the nucleus.

Coherent pion production processes induced by neutrinos and antineutrinos on nuclei via. charged and neutral currents have been the subject of intense studies in the last few years. The

https://doi.org/10.1017/9781108489065.016 Published online by Cambridge University Press

coherent pion production process

$$\nu_l\,(\bar{\nu}_l)\;+\;\mathcal{A}\;\rightarrow\;l^{\mp}\,(\nu_l/\bar{\nu}_l)\;+\;\mathcal{A}\;+\;\pi^{\pm}(\pi^0), \tag{15.32}$$

can be qualitatively interpreted as the emission of a virtual pion from the weak interaction of neutrino followed by the elastic scattering of this off-shell pion with the target nucleus till it becomes a real pion and the target nucleus remains in the ground state. In the coherent interactions on nuclei, the overall scattering amplitude is given as the sum of the constructive interference between the scattering amplitudes of the incident wave on the various nucleons in the target nucleus, which implies that all the nucleons in the nucleus must react in phase in order to have maximum constructive interferences for enhanced cross section. Thus, the momentum transferred ($|\vec{k}|$) to any nucleons in a nucleus of radius (R) must thus be small enough so that the condition

$$|\vec{k}|R\;<\;1. \tag{15.33}$$

gets fulfilled, implying that the nucleons remain bound in the nucleus.

Coherent reactions are also characterized by the fact that the target nucleus recoils as a whole without breaking up with very little recoil energy since the effect of the incident wave is approximately the same on all the nucleons; otherwise, the coherence would disappear. In coherent interactions, enhanced cross section can occur due to the coherence effect as long as no charge, spin, isospin or any other additive quantum number is transferred to the target nucleus. If any of these are forbidden, then this would single out a specific nucleon, and destroy the coherence. For example, the total isospin (I) of the exchanged state must be zero. Indeed, the operator I_3 induced amplitude for protons and neutrons would have an opposite sign, resulting in a small effect on the nuclei with total isospin $I = 0$. If the nucleus has spin, the spin term in the coherent amplitude are suppressed in comparison to the total spin zero nuclei. Moreover, the emission of scattered particles in the forward direction, which is generally the case, implies that the coherent interactions conserve helicity.

Coherent production of pions induced by neutrinos and antineutrinos on nuclei have been reported in four possible charged as well as neutral current channels (Figure 15.2):

$$\left.\begin{array}{l}\nu_\mu\;+\;\mathcal{A}\;\rightarrow\;\mu^-\;+\;\mathcal{A}\;+\;\pi^+\\ \bar{\nu}_\mu\;+\;\mathcal{A}\;\rightarrow\;\mu^+\;+\;\mathcal{A}\;+\;\pi^-\end{array}\right\}\quad\text{(Charged current)} \tag{15.34}$$

$$\left.\begin{array}{l}\nu_\mu\;+\;\mathcal{A}\;\rightarrow\;\nu_\mu\;+\;\mathcal{A}\;+\;\pi^0\\ \bar{\nu}_\mu\;+\;\mathcal{A}\;\rightarrow\;\bar{\nu}_\mu\;+\;\mathcal{A}\;+\;\pi^0\end{array}\right\}\quad\text{(Neutral current)} \tag{15.35}$$

These processes can be studied in detail and with relatively large statistics and small background as the kinematical situation in coherent processes are different from other interaction processes and also due to the small pion mass and simple geometry. Experimentally, the coherent charged as well as neutral current pion production induced by neutrinos and antineutrinos have been

https://doi.org/10.1017/9781108489065.016 Published online by Cambridge University Press

observed on various nuclei using different techniques such as bubble chambers and spark chambers [704]–[709]. The events are characterized by the small four-momentum transfer to the nucleus and the exponential fall of the cross section with $|t|$, where $t = (q - p_\pi)^2$, $q = k - k'$. The nucleus remains undetected experimentally, but it can be estimated from the measurement of the muon and meson momenta.

In addition to $|t|$ dependence, coherent scattering also depends on the square of the four-momentum (Q^2) transferred between the leptons. Experimentally, it has also been established that the coherent scattering cross section peaks at low $Q^2 (\leq 0.1\ \text{GeV}^2)$ and the cross section rises as a function of neutrino energy which becomes logarithmic at large neutrino energies. In

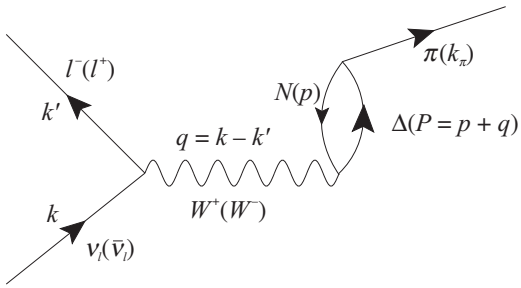

Figure 15.2 Feynman diagram considered for coherent pion production through $\Delta - h$ excitation. In the charged current reaction, k' is the four-momentum of the charged lepton, and $q(= k - k')$ is the four-momentum of the $W^{\pm}$ boson. In the neutral current reaction, k' is the momentum of the scattered neutrino and q is the momentum of the exchanged Z^0.

this sense, the neutrino induced coherent pion production reaction has an advantage over other existing reactions, which can enrich our understanding of the nuclear excitation mechanism; it also allows the study of the longitudinal axial vector current for very small Q^2 values, providing the most detailed test of the PCAC hypothesis at high energies. A good knowledge of coherent pion production induced by neutrinos and antineutrinos is also important in understanding the background of the quasielastic lepton production in the forward direction in the analysis of neutrino oscillation experiments with atmospheric and accelerator neutrino beams in intermediate energies. There are two approaches which have been used to calculate coherent pion production cross section:

(i) methods based on PCAC, and

(ii) microscopic models using nuclear structure.

15.3.2 PCAC based methods

Coherent pion production cross section can be calculated using Adler's theorem [753] relating the inelastic neutrino scattering cross section in the forward direction with pion nucleus scattering. In the forward direction, that is, $\theta = 0$, the initial and final leptons are produced in parallel configurations, that is, the initial and final momenta of leptons $\vec{k}$ and $\vec{k'}$ are parallel to each other. In the limit of $m_l \to 0$, the momentum transfer square $q^2 (= (k - k')^2) \approx 0$ and all

https://doi.org/10.1017/9781108489065.016 Published online by Cambridge University Press

the momenta k^μ, k'^μ, and q^μ are null vectors and $\vec{k}, \vec{k'}$, and $\vec{q}$ are colinear. Moreover, in the case of an inelastic reaction like $\nu + N \rightarrow \mu^- + X$, the mass of final hadron $M_X \neq M$ making $q_0 \neq 0$. A simple algebra shows that in this kinematic configuration, the momenta k^μ and k'^μ are proportional to each other and also to q^μ; thus, we can write [753]

$$k'^\mu = \frac{k' \cdot p}{q \cdot p} q^\mu \qquad k^\mu = \frac{k \cdot p}{q \cdot p} q^\mu. \tag{15.36}$$

We also know that in any neutrino reaction, the cross section $d\sigma$ is proportional to the product of leptonic and hadronic tensors, that is,

$$d\sigma \quad \propto \quad \sum_{\text{spin}} L^{\mu\nu} \langle X|J_\mu|N\rangle \langle X|J_\nu|N\rangle^*,$$

where $L^{\mu\nu} \propto k^\mu k'^\mu + k'^\mu k^\nu - g^{\mu\nu} k \cdot k' + i\epsilon^{\mu\nu\rho\sigma} k_\rho k'_\sigma$.

Since k^μ and k'^μ are now proportional to q^μ, $d\sigma$ becomes proportional to $q^\mu q^\nu$:

$$d\sigma \quad \propto \quad \langle X|q^\mu J_\mu|N\rangle \langle X|q^\nu J_\nu|N\rangle^*. \tag{15.37}$$

Using the hypothesis of CVC and PCAC, we obtain

$$q^\mu V_\mu = 0, \qquad q^\mu A_\mu = f_\pi m_\pi^2 \phi_\pi. \tag{15.38}$$

Therefore, the amplitude $q^\mu A_\mu$ is related to the matrix element of the pion field taken between $|N\rangle$ and $|X\rangle$ states, that is,

$$\langle X|q^\mu A_\mu|N\rangle = \frac{f_\pi m_\pi^2}{q^2 - m_\pi^2} T(\pi^\alpha N \rightarrow X) \tag{15.39}$$

in the pion pole approximation. We see that the matrix element for the transition $\nu + n \rightarrow \mu^- + X$ through the weak current J_μ gets nonzero contribution only from the divergence of the axial vector current (i.e., $q_\mu A^\mu$) in the $q^2 \approx 0$ limit which is related with the pion nucleon scattering corresponding to $q^2 = 0$ and $q_0 = E_\pi$ limit in the case of single pion production.

In this approximation, Adler obtained the expression of cross section for the reaction $\nu + N \rightarrow \mu^- + N + \pi^\alpha$ in the limit of $q^2 = 0$. This expression was used by Rein and Sehgal [715] to calculate the coherent production of π^0 from nuclei by extending it to $q^2 \neq 0$ values. Adler's formula is expressed as [753]

$$\frac{d\sigma}{dq^2 dy dt} = r \frac{G_F^2 f_\pi^2}{2\pi^2} \frac{(1-y)}{y} \frac{d\sigma}{dt}(\pi A \rightarrow \pi A_{gs})\Big|_{q^2=0, q_0=E_\pi} \tag{15.40}$$

with $r = 2\cos\theta_C(1)$ for the CC (NC) reaction. $t = (q - p_\pi)^2$ and $y = \frac{q_0}{E_\nu}$. $\frac{d\sigma}{dt}(\pi A \rightarrow \pi A_{gs})$ is the cross section for the pion nucleus scattering neglecting the nucleus recoil (i.e., $q_0 = E_\pi$). Rein and Sehgal [715] used a form factor $F(q^2) = \frac{1}{\left(1 - \frac{q^2}{M_A^2}\right)^2}$ to extend it to $q^2 \neq 0$ and the following expression for the pion–nucleus scattering cross section was used [761]:

$$\frac{d\sigma}{dt}(\pi A \rightarrow \pi A_{g.s.}) = \frac{d\sigma}{dt} = |F_A(t)|^2 F_{\text{abs}} \frac{d\sigma}{dt}(\pi N \rightarrow \pi N)\Big|_{t=0},$$
$$\text{where } F_A(t) = \int d^3 r e^{i(\vec{q} - \vec{p}_\pi)\cdot\vec{r}} (\rho_p(r) + \rho_n(r)). \tag{15.41}$$

https://doi.org/10.1017/9781108489065.016 Published online by Cambridge University Press

where $\frac{d\sigma}{dt}(\pi N \rightarrow \pi N)$ is the pion nucleon cross section and F_{abs} is the factor describing the absorption of pions. This has been used in most of the early versions of neutrino events generators. Since then, many authors have extended and updated the formula by including the following corrections to the coherent pion production:

i) Lepton mass correction due to $m_l \neq 0$ relevant for charge current reactions.
ii) Improved kinematic and dynamic corrections due to $q^2 \neq 0$.
iii) Including the contribution of other mesons in addition to the pion pole as done in Adler's model and used by Rein and Sehgal [715].
iv) Improved treatment of pion nucleus cross section relevant to the experimental kinematics of present neutrino experiments.

These corrections led to reduction in the cross section as predicted by the Rein and Sehgal model [715] and are similar to those obtained with other methods using microscopic models.

15.4 Microscopic Model for Coherent Weak Pion Production

The amplitude for the charged current weak pion production from the nuclei for the delta pole term corresponding to the Feynman diagrams shown in Figure 15.3, is written in terms of l^μ, the leptonic current and hadronic current $\mathcal{J}^\mu = J_s^\mu + J_u^\mu$ as the sum of direct (s channel) and crossed (u channel) diagrams and a nuclear form factor as.

$$\mathcal{A} = \frac{G_F}{\sqrt{2}} \cos\theta_C \, l^\mu \, \mathcal{J}_\mu \, \mathcal{F}(\vec{q} - \vec{k}_\pi), \tag{15.42}$$

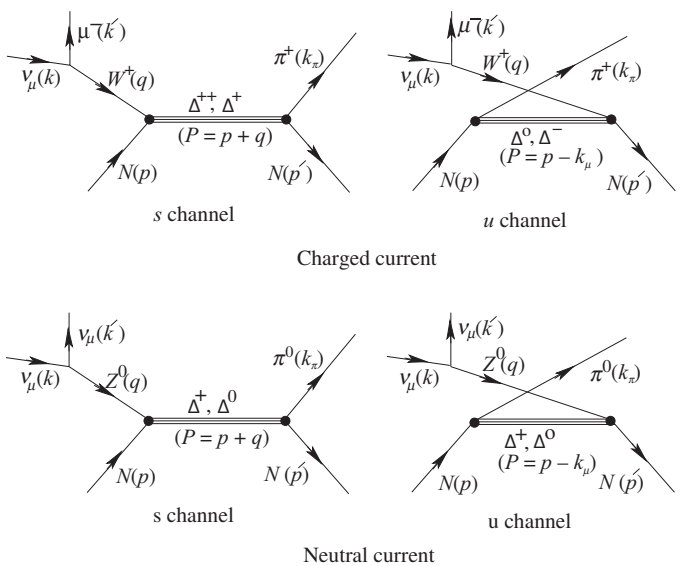

Figure 15.3 Feynman diagrams considered for neutrino induced weak coherent pion production for Δ-resonance.

https://doi.org/10.1017/9781108489065.016 Published online by Cambridge University Press

where G_F is the Fermi coupling constant and $\mathcal{F}(\vec{q}-\vec{k}_\pi)$ is the nuclear form factor including the isospin factors.

The hadronic current for the s channel process using Feynman rules may be written as

$$J_s^\mu \;=\; \sqrt{3}\,\frac{f_{\pi N\Delta}}{m_\pi}\,k_\pi^\sigma\,\sum_r \bar{u}_r(p')\,\Delta_{\sigma\lambda}\,\mathcal{O}^{\lambda\mu}\,u_r(p). \tag{15.43}$$

The operators $\Delta_{\sigma\lambda}$ and $O^{\lambda\mu}$ are discussed in Chapters 11 and 12.

Similarly, one may write the hadronic current for the u channel process.

For the coherent process, we write the spinors in the rest frame of the nucleus in the following form

$$u_r(\vec{p}) \;=\; \frac{\not{p}+M}{\sqrt{2M(E+M)}}u_r(0), \tag{15.44}$$

$$\bar{u}_r(\vec{p}') \;=\; \bar{u}_r(0)\frac{\not{p}'+M}{\sqrt{2M(E'+M)}}, \tag{15.45}$$

$$\sum_r u_r(0)\bar{u}_r(0) \;=\; \frac{1+\gamma_0}{2}. \tag{15.46}$$

Considering only $C_5^A(Q^2)$ which is the most dominant term in $O^{\lambda\mu}$, J_μ^s may be written as

$$J_\mu^s \;=\; \chi\,\mathrm{Tr}\left[(1+\gamma_0)\,(\not{p}+M)\,(\not{p}'+M)\,k_\sigma^\pi\,(\not{P}+M_\Delta)\left(g^{\sigma\lambda}-\frac{1}{3}\gamma^\sigma\gamma^\lambda-\frac{2}{3M_\Delta^2}P^\sigma P^\lambda + \frac{P^\sigma\gamma^\lambda-\gamma^\sigma P^\lambda}{3M_\Delta}\right)g_{\lambda\mu}\right] \tag{15.47}$$

with

$$\chi = \sqrt{3}\left(\frac{f_{\pi N\Delta}}{m_\pi}\right)\left(\frac{1}{2}\right)^2\left(\frac{1}{2M}\right)^2\frac{C_5^A(Q^2)}{(P^2-M_\Delta^2)+i\Gamma M_\Delta}$$

Using trace algebra, we find the final expression as

$$J_\mu^s = 8\,\chi\,\left[\alpha_s\,k_\mu^\pi+\beta_s\,P_\mu+\gamma_s\,p_\mu\right], \tag{15.48}$$

where α_s, β_s, and γ_s are the coefficients associated with k_μ, P_μ, and p_μ respectively that can be obtained after the trace calculation.

The nuclear form factor $\mathcal{F}(\vec{q}-\vec{k}_\pi)$ is given as

$$\mathcal{F}(\vec{q}-\vec{k}_\pi) = \int d^3r\,\rho(\vec{r})\,e^{-i(\vec{q}-\vec{k}_\pi).\vec{r}}, \tag{15.49}$$

with $\rho(\vec{r})$ as the nuclear matter density which is a function of nucleon relative coordinates. It is the linear combination of proton and neutron densities incorporating the isospin factors.

https://doi.org/10.1017/9781108489065.016 Published online by Cambridge University Press

15.4.1 Cross sections

The differential cross section for a pion produced in the charged current weak production process induced by neutrinos can be written as

$$\left[\frac{d^5\sigma}{dE_\pi d\Omega_\pi dQ^2}\right]_{CC} = \frac{\pi}{8}\frac{1}{(2\pi)^5}\frac{M}{E_k^2}\,|\,\vec{k}_\pi|\,\frac{1}{\mathcal{R}}\,\overline{\sum}\sum|\mathcal{A}|^2, \tag{15.50}$$

where

$$\mathcal{R} \;=\; \left[\left(E_{p'} + E_{k'} - E_k\cos\theta_{kk'}\right) - \frac{|\vec{k_\pi}|}{|\vec{q}|}\left(E_{k'} - E_k\cos\theta_{kk'}\right)\cos\theta_{\pi q}\right] \tag{15.51}$$

is a kinematical factor incorporating the recoil effects, which is very close to unity for low $Q^2(=-q^2)$, relevant for coherent reactions.

We find that the recoil of the nucleus gives less than $(3-4\%)$ correction in the energy region of around 1 GeV. In the charged current weak reaction, we could also measure the energy and the momentum of the leptons. It also allows an approximate separation of the coherent cross section from the non-coherent background. We can measure the differential cross section for the charged lepton production,

$$\left(\frac{d^5\sigma}{d\Omega_\pi d\Omega_{kk'}dE'_k}\right)_{CC} \;=\; \frac{1}{8}\frac{1}{(2\pi)^5}\frac{|\,\vec{k'}|\,|\,\vec{k}_\pi|}{E_k}\,\mathcal{R}\,\overline{\sum}\sum|\mathcal{A}|^2 \tag{15.52}$$

where

$$\mathcal{R} = \left[\frac{M\,|\vec{k}_\pi|}{E_{p'}|\vec{k}_\pi| + E_\pi(|\vec{k}_\pi| - |\vec{q}|\cos\theta_{\pi q})}\right] \tag{15.53}$$

15.4.2 Final state interactions

The pions which are produced in these processes while traveling inside the nucleus, can be absorbed, can change direction, energy, charge, or even produce more pions due to various processes like elastic and charge exchange scattering with the nucleons present in the nucleus through strong interactions. Therefore, the production cross sections for the pions from the nuclear targets are affected by the presence of strong interactions of the final state pions in the nuclear medium (Figure 15.4). For example, a pion produced in the nuclear medium may get absorbed by the nucleons and thus, mimick a quasielastic-like event (see Figure 15.5).

There are many approaches developed initially in the inelastic production of pions from electron–nucleus and proton–nucleus scattering which can be applied to (anti)neutrino–nucleus scattering. The various processes which affect the pions after they are produced are pion absorption, elastic and charge exchange scattering of pions. The earlier calculations of the

https://doi.org/10.1017/9781108489065.016 Published online by Cambridge University Press

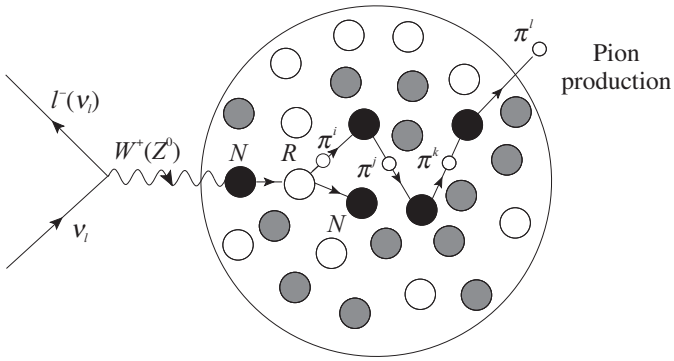

Figure 15.4 Pion production inside a nuclear target and its interaction with the nucleons in the nucleus while coming out. The pions may undergo elastic scattering, charge exchange (for example, $\pi^+ + n \rightarrow \pi^0 + p$) reaction, etc. and therefore, the charge of the pion may change along the way before it comes out of the nucleus. Circles have the same meaning as in Figure 15.1.

final state interactions (FSI) of pions applied to $\nu(\bar{\nu})$ scattering from nucleons were done by Adler et al. [753], who used a multipole scattering theory of pions. The other methods use the approach of distorted wave Born approximation (DWBA) in which the plane wave pion is replaced by a distorted pion wave obtained by solving the Klein–Gordon equation for pions in an optical potential [762]. In case of high energy and forward angles corresponding to a very low q^2 relevant for the coherent production, the Glauber model for calculating the pion distortion is most appropriate [720, 763]. In a microscopic approach, the pion trajectory is traced within the nucleus from its point of production, weighted by the probability for various final state interactions like its absorption, elastic scattering, and charge exchange scattering with the nucleon until it comes out of the nucleus. This is the method used in most of the neutrino event generators like NUANCE and NEUT; it is used even today in modern neutrino event generators. In the following, we outline the basic ingredients of the last two methods.

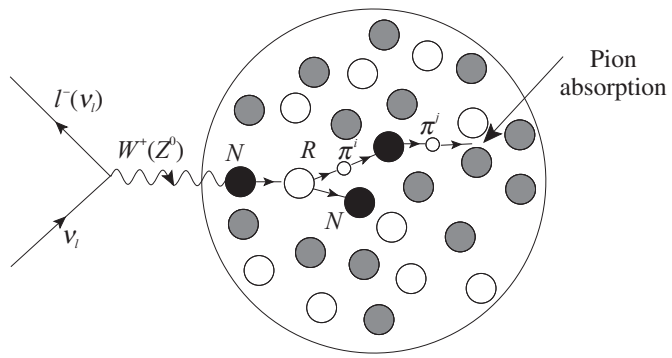

Figure 15.5 A neutrino induced reaction on a nucleon target when a pion is absorbed in the nuclear medium while coming out. Circles have the same meaning as in Figure 15.1.

https://doi.org/10.1017/9781108489065.016 Published online by Cambridge University Press

FSI in Glauber model

The pions produced in these processes inside the nuclear medium may rescatter or may produce more pions or may get absorbed while coming out from the final nucleus. The pion absorption is a relatively small effect at high energies. However, at lower energies there are considerable number of pions affected by the quasielastic rescattering and further pion production on the nuclear nucleons. The proportion of the pions that eventually comes out of the nucleus is essentially determined by the absorption strength.

We have considered the final state interaction of the pion by replacing the plane wave pion by a distorted wave pion. The distortion of the pion wave is calculated using the Eikonal approximation of Glauber [764] in the impact parameter representation (Figure 15.6). The nuclear form factor $\mathcal{F}(\vec{q}-\vec{k}_\pi)$, in impact parameter representation may be written as

$$\mathcal{F}(\vec{q}-\vec{k}_\pi) = \int d^2b dz\, \rho(\vec{b},z)\, e^{i(\vec{q}-\vec{k}_\pi)\cdot(\vec{b}+\hat{q}z)} \tag{15.54}$$

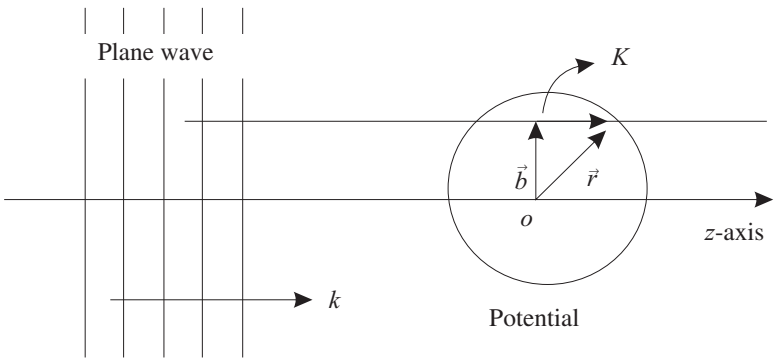

Figure 15.6 Definition of impact parameter in scattering processes at high energies. We choose the z-axis to lie in the direction of propagation of $\vec{k}$ and $\vec{K} = \vec{k} + \vec{k}'$.

where d^2b denotes the integration over the plane of impact vector. $\vec{r} = (\vec{b},z)$, and $\vec{q}$ the momentum transfer is chosen to be along the z direction. With this choice, the exponential factor becomes

$$e^{i(\vec{q}-\vec{k}_\pi)\cdot(\vec{b}+\hat{q}z)} = e^{-i\vec{k}^t_\pi\cdot\vec{b}}\, e^{i(|\vec{q}|-k^l_\pi)z}$$

where $\vec{k}^t_\pi$ and $k^l_\pi = \vec{k}_\pi\cdot\hat{q} = \frac{\vec{k}_\pi\cdot\vec{q}}{|\vec{q}|}$ are the transverse and longitudinal components of the pion momentum. Moreover, for the potential with azimuthal symmetry, we may carry the ϕ integration by noting that $\frac{1}{2\pi}\int_0^{2\pi} e^{i\lambda\cos\phi}d\phi = J_0(\lambda)$, where $J_0(\lambda)$ is the zeroth order Bessel's function. Finally, we may write $\mathcal{F}(\vec{q}-\vec{k}_\pi)$

$$\mathcal{F}(\vec{q}-\vec{k}_\pi) = 2\pi\int_0^\infty b\, db \int_{-\infty}^\infty dz\, \rho(\vec{b},z)\, J_0(k^t_\pi b)\, e^{i(|\vec{q}|-k^l_\pi)z}\, e^{-if(\vec{b},z)} \tag{15.55}$$

https://doi.org/10.1017/9781108489065.016 Published online by Cambridge University Press

where

$$f(\vec{b},z) = \int_z^\infty \frac{1}{2|\vec{k}_\pi|}\Pi(\rho(\vec{b},z'))dz' \tag{15.56}$$

and the pion self energy Π related to the pion optical potential $V_{opt}(E_\pi,\vec{r})$ as $\Pi(\rho(\vec{r})) = 2E_\pi V_{opt}(E_\pi,\vec{r})$ is defined as

$$\Pi(\rho) = \frac{4}{9}\left(\frac{f_{\pi N\Delta}}{m_\pi}\right)^2 \frac{M^2}{W^2}|\vec{p}_\pi|^2\rho\frac{1}{W - \widetilde{M}_\Delta + \frac{i\widetilde{\Gamma}}{2}}. \tag{15.57}$$

Microscopic model of pion propagation

Now, we will describe in brief the prescription of Vicente Vacas [765] which we have followed while presenting the numerical results for the incoherent one pion production with FSI. In this prescription, a pion of given momentum and charge is moved along the z-direction with a random impact parameter $\vec{b}$, with $|\vec{b}| < R$, where R is the nuclear radius which is taken to be a point where nuclear density $\rho(R)$ falls to $10^{-3}\rho_0$, and ρ_0 is the central density. To start with, the pion is placed at a point $(\vec{b},z_{in})$, where $z_{in} = -\sqrt{R^2 - |\vec{b}|^2}$ and then it is moved in small steps δl along the z-direction until it comes out of the nucleus or interacts with the nucleon. If $P(k_\pi,r,\lambda)$ is the probability per unit length at the point r of a pion of momentum $\vec{k}_\pi$ and charge λ, then $P\delta l << 1$. A random number x is generated such that $x \in [0,1]$ and if $x > P\delta l$, then it is assumed that the pion has not interacted while traveling a distance δl. However, if $x < P\delta l$, then the pion has interacted and depending upon the weight factor of each channel given by its cross section, it is decided if the interaction is quasielastic, charge exchange reaction, pion production, or pion absorption. For example, for the quasielastic scattering

$$P_{N(\pi^\lambda,\pi^{\lambda'})N'} = \sigma_{N(\pi^\lambda,\pi^{\lambda'})N'} \times \rho_N(r),$$

where N is a nucleon, ρ_N is its density, and σ is the elementary cross section for the reaction $\pi^\lambda + N \to \pi^{\lambda'} + N'$ obtained from the phase shift analysis.

For a pion to be absorbed, P is expressed in terms of the imaginary part of the pion self energy Π, that is, $P_{abs} = -\frac{Im\Pi_{abs}(k_\pi)}{k_\pi}$, where the self energy Π is related to the pion optical potential V.

15.5 Results for Cross Sections

(i) Incoherent pion production

In Figure 15.7, the results for Q^2-distribution $\frac{d\sigma}{dQ^2}$ and momentum distribution $\frac{d\sigma}{dp_\pi}$ are shown for the charged current $\nu_\mu(\bar{\nu}_\mu)$ induced incoherent one π^+ (π^-) production cross section. These results are presented for the differential scattering cross section calculated with and without the nuclear medium effects and with nuclear medium effects including the pion

https://doi.org/10.1017/9781108489065.016 Published online by Cambridge University Press

absorption effects. For the Q^2-distribution shown in Figure 15.7, we see that the reduction in the cross section as compared to the cross section calculated without the nuclear medium effects is around 35% in the peak region. When pion absorption effects are also taken into

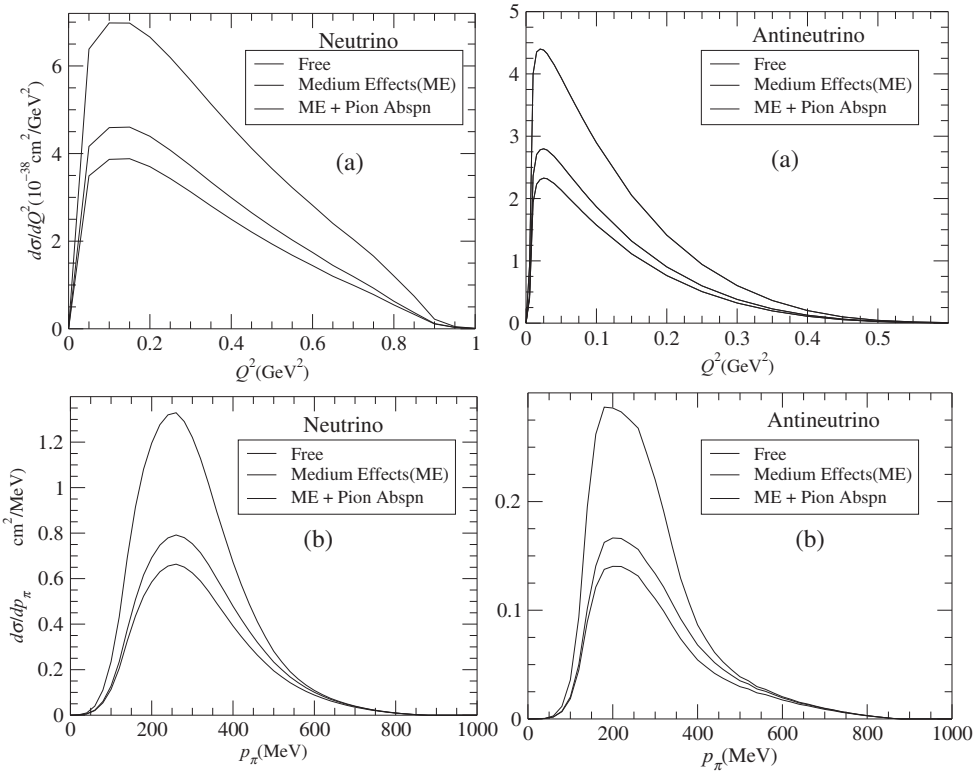

Figure 15.7 $\frac{d\sigma}{dQ^2}$ and $\frac{d\sigma}{dp_\pi}$ for the $\nu_\mu(\bar{\nu}_\mu)$ induced charged current one $\pi^+(\pi^-)$ process on ^{12}C target at $E_\nu = 1$ GeV [766].

account, there is a further reduction of around 15%. The results for the antineutrino induced one π^- production cross section are qualitatively similar in nature but quantitatively, we find that the peak shifts toward a slightly lower value of Q^2. In Figure 15.7, the results for the pion momentum distribution have been shown. In this case, the reduction in the cross section in the peak region is around 40% when nuclear medium effects are taken into account, which further reduces by about 15% when pion absorption effects are also taken into account.

In Figure 15.8, the results for the total scattering cross section σ for charged current $\nu_\mu(\bar{\nu}_\mu)$ induced one $\pi^+(\pi^-)$ production cross section are shown. We see that with the inclusion of nuclear medium effects, the reduction in the cross section from the cross section calculated without the nuclear medium effects for neutrino energies between 1–2 GeV is 30–35%, which further reduces by 15% when pion absorption effects are also taken into account. The results with antineutrinos are similar in nature.

https://doi.org/10.1017/9781108489065.016 Published online by Cambridge University Press

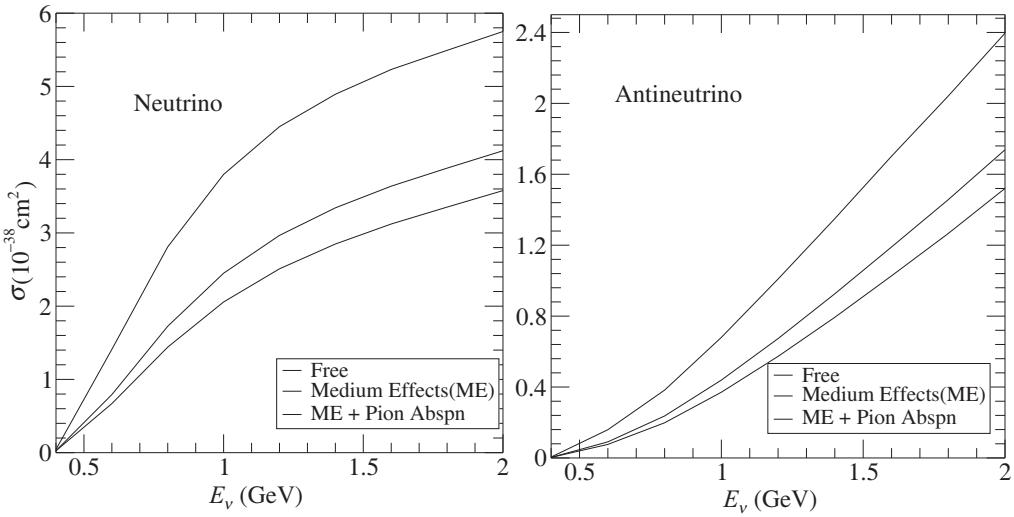

Figure 15.8 σ for ν_μ ($\bar{\nu}_\mu$) induced charged current incoherent $\pi^+(\pi^-)$ production on ^{12}C target [766].

Figure 15.9 shows the pion kinetic energy distribution $\frac{d\sigma}{dT}$ in the CC $1\pi^+$, ν_μ induced interaction on CH_2 obtained in the MiniBooNE [767] experiment. In the top panel, comparison

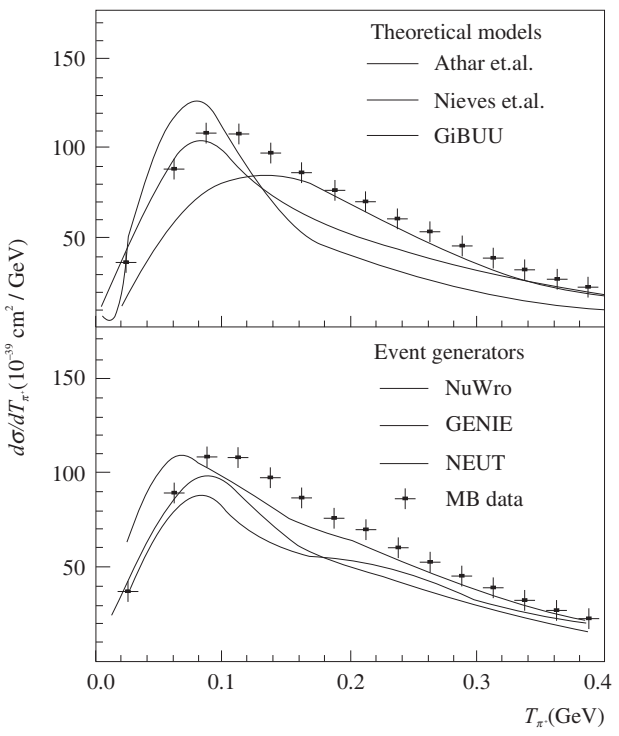

Figure 15.9 Comparison of theoretical and event generator calculations for the differential cross sections in pion kinetic energy with the MiniBooNE [767] ν_μ CH_2 CC $1\pi^+$ production data [768].

https://doi.org/10.1017/9781108489065.016 Published online by Cambridge University Press

has been made with the theoretical calculations of Athar et al. [668, 727] and Nieves et al. [692] as well as with the GiBUU MC generator [769]. In the lower panel, comparison has been made with the other MC generators like NEUT [607], GENIE [606], and NuWro [728]. These results were compiled by Rodrigues [768].

(ii) Coherent pion production

In Figure 15.10, results are presented for the total scattering cross section (σ^{CC}) for a coherent charged current reaction induced by ν_μ in ^{12}C [763]. The results for $\sigma^{CC}(E_\nu)$ (scaled by a factor of $\frac{1}{2}$) vs. E_ν are shown without nuclear medium effects and with nuclear medium effects. When the pion absorption and nuclear medium effects are both taken into account, the results for $\sigma^{CC}(E_\nu)$ are shown by solid lines. We see that the nuclear medium effects lead to a reduction of 30–35% around E_ν=1–1.5 GeV in $\sigma^{CC}(E_\nu)$ while the reduction due to the final state interaction is quite large. Also shown in this figure are the results for $\sigma^{CC}(E_\nu)$ vs. E_ν when a cut of 450 MeV is applied on the muon momentum as done in the K2K experiment [746]; the theoretical results [763] are found to be consistent with the data.

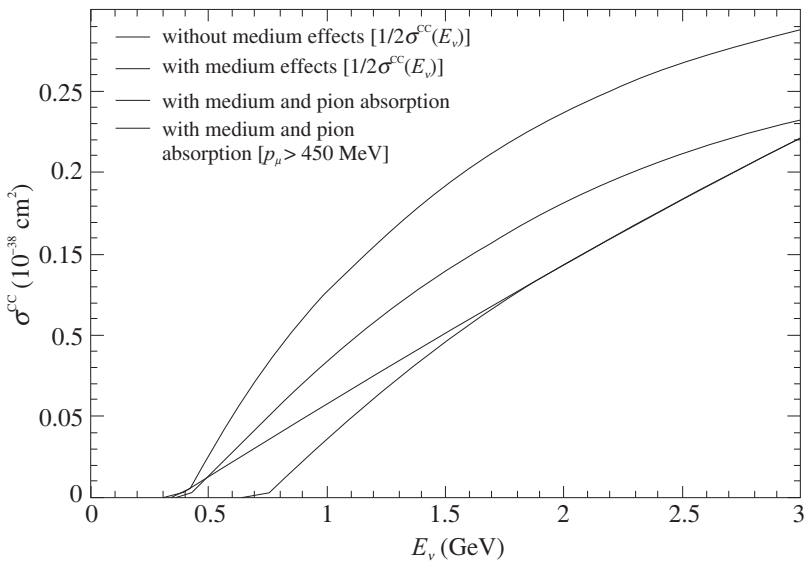

Figure 15.10 $\sigma(E_\nu)$ vs. E_ν for coherent π^+ production in ^{12}C

To conclude:

(i) the contribution to the cross section comes mainly from the s-channel diagram ($> 90\%$) which is dominated by the on shell Δ, thus making the off shell correction quite small.

(ii) the contribution to the cross section from the vector current is negligibly small (<2 %); the major contribution comes from the axial current only, leading to near equality of neutrino and antineutrino cross sections.

https://doi.org/10.1017/9781108489065.016 Published online by Cambridge University Press

The differential cross sections $\frac{d\sigma}{dq^2}$ and $\frac{d\sigma}{dk_\pi}$ for charged pion production at $E_\nu = 1$ GeV are presented in Figures.15.11, where nuclear medium and final state interactions effects are shown explicitly. In the inset, we exhibit the differential cross sections $< \frac{d\sigma}{dq^2} >$ and $< \frac{d\sigma}{dk_\pi} >$ averaged over the K2K and MiniBooNE neutrino spectra without applying any cuts on the muon momentum.

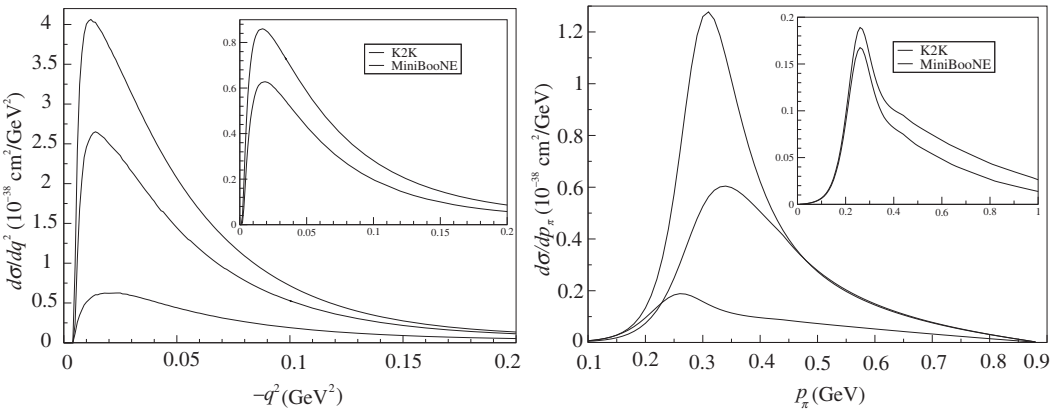

Figure 15.11 (a) $\frac{d\sigma}{dq^2}$ *vs.* $-q^2$ at E_ν=1 GeV, for coherent π^+ production in ^{12}C nucleus without(dotted), with(dashed) nuclear medium effects and with nuclear medium and pion absorption effects (solid). In the inset, the final results for $< \frac{d\sigma}{dq^2}$ vs. $-q^2$ averaged over the K2K and MiniBooNE spectrum are shown. (b) $\frac{d\sigma}{dk_\pi}$ *vs.* k_π at E_ν=1 GeV.

In an improved calculation, Alvarez-Ruso et al. [770] have also included the contribution of the non-resonant diagram; it has been found that these contributions are very small at $E_\nu \sim 1$ GeV.

15.6 Pion Production through Hyperon Excitation

The $\Delta S = 1$ hyperon (Y) production processes induced by antineutrinos producing pions are given by (Chapter 10 for detail)

$$\bar{\nu}_l(k) + N(p) \to l^+(k') + Y(p') \\ \hookrightarrow N'(p') + \pi(k_\pi), \tag{15.58}$$

where $Y = \Lambda, \Sigma^{0,-}$. The differential scattering cross section for this process in the laboratory frame may be written as

$$d\sigma = \frac{\delta^4(k + p - k' - p')}{16\pi^2 E_\nu M_N} \frac{d^3k'}{2E_{k'}} \frac{d^3p'}{2E_{p'}} \sum\overline{\sum} |\mathcal{M}|^2, \tag{15.59}$$

https://doi.org/10.1017/9781108489065.016 Published online by Cambridge University Press

where M_N is the nucleon mass and $\mathcal{M}$ is the matrix element written as

$$\mathcal{M} = \frac{G_F}{\sqrt{2}} \sin\theta_c \bar{v}_l(k')\gamma^\mu(1-\gamma^5)v_\nu(k)\, J_\mu, \tag{15.60}$$

where J_μ is the hadronic current, which is written as

$$J_\mu = \bar{u}_Y(p')\left[\gamma_\mu f_1(q^2) + i\sigma_{\mu\nu}\frac{q^\nu}{M+M_Y} f_2(q^2) - \gamma_\mu\gamma_5 g_1(q^2) - \frac{q_\mu}{M_Y}\gamma_5 g_3(q^2)\right] u_N(p) \tag{15.61}$$

where $f_i(q^2)$ $(i = 1,2)$ and $g_i(q^2)$ $(i = 1,3)$ are the vector and axial vector $N - Y(Y = \Lambda, \Sigma^-, \Sigma^0)$ transition form factors, respectively, which are given in terms of the functions $F_i^V(q^2)$ and $D_i^V(q^2)$ corresponding to vector couplings and $F_i^A(q^2)$ and $D_i^A(q^2)$ corresponding to axial vector couplings (Chapter 10).

When the reactions shown in Eq. (15.58) take place on nucleons in the nucleus, Fermi motion and Pauli blocking effects of initial nucleons are considered. The Fermi motion effects are calculated in a local Fermi gas model, and the cross section is evaluated as a function of local Fermi momentum $p_F(r)$ and integrated over the whole nucleus. The differential scattering cross section in this model is given by

$$\frac{d\sigma}{dQ^2 dE_l} = 2\int d^3r \int \frac{d^3p}{(2\pi)^3} n_N(p,r)\left[\frac{d\sigma}{dQ^2 dE_l}\right]_{\text{free}}, \tag{15.62}$$

where $n_N(p,r)$ is the occupation number of the nucleon.

The produced hyperons are affected by the FSI within the nucleus through the hyperon–nucleon quasielastic and charge exchange scattering processes like $\Lambda + n \to \Sigma^- + p$, $\Lambda + n \to \Sigma^0 + n$, $\Sigma^- + p \to \Lambda + n$, $\Sigma^- + p \to \Sigma^0 + n$, etc. Because of such types of interaction in the nucleus, the probability of Λ or Σ production changes; this has been taken into account by using the prescription given in Ref. [771]. In this prescription, an initial hyperon produced at a position r within the nucleus interacts with a nucleon to produce a new hyperon state within a short distance dl with a probability $P = P_Y dl$, where P_Y is the probability per unit length given by

$$P_Y = \sigma_{Y+n\to f}(E)\,\rho_n(r) \;+\; \sigma_{Y+p\to f}(E)\,\rho_p(r),$$

where f denotes a possible final hyperon–nucleon $[Y_f(\Sigma \text{ or } \Lambda) + N(n \text{ or } p)]$ state with energy E in the hyperon–nucleon center of mass system, $\rho_n(r)[\rho_p(r)]$ is the local density of the neutron(proton) in the nucleus, and σ is the total cross section for a charged current channel like $Y(\Sigma \text{ or } \Lambda) + N(n \text{ or } p) \to f$ [771]. Now a particular channel is selected, which gives rise to a hyperon Y_f in the final state with the probability P. For the selected channel, the Pauli blocking effect is taken into account by first randomly selecting a nucleon in the local Fermi sea. Then a random scattering angle is generated in the hyperon–nucleon center of mass system

https://doi.org/10.1017/9781108489065.016 Published online by Cambridge University Press

assuming the cross sections to be isotropic. Using this information, the hyperon and nucleon momenta are calculated and the Lorentz boosted to the lab frame. If the nucleon in the final state has momenta above the Fermi momenta, we have a new hyperon type (Y_f) and/or a new direction and energy of the initial hyperon (Y_i). This process is continued until the hyperon gets out of the nucleus. The decay modes of hyperons to pions is highly suppressed in the nuclear medium [772], making them live long enough to pass through the nucleus and decay outside the nuclear medium. Therefore, the produced pions are less affected by the strong interaction of the nuclear field; their FSI have not been taken into account.

In Figure 15.12, the results for the cross sections $\sigma(E_{\bar{\nu}})$ for one pion production obtained from the hyperon excitation and the Δ excitation are compared. These results are presented with

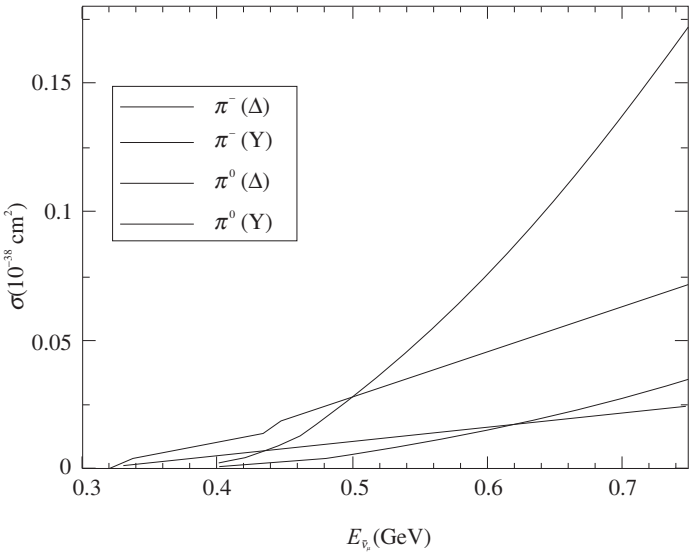

Figure 15.12 $\sigma(E_{\bar{\nu}_\mu})$ vs. $E_{\bar{\nu}_\mu}$ for π^- & π^0 production in ^{12}C, in the Δ dominance model and via intermediate hyperons.

the nuclear medium and FSI effects for the pions interacting with the residual nucleus for π^- as well as π^0 productions obtained in the delta dominance model and the pions obtained from the hyperons where the medium effects in hyperon production and FSI due to hyperon–nucleon interaction in the nuclear medium have been taken into account. When the results for the cross sections are compared in these two processes, we see that, at lower antineutrino energies $E_{\bar{\nu}} <$ 500 MeV, the contribution of π^- from the hyperon excitation is more than the pions coming from the Δ excitation. For $E_{\bar{\nu}} > 500$ MeV, the contribution from Δ excitation starts dominating and at $E_{\bar{\nu}} = 1$ GeV, the contribution of π^- from the hyperon excitation is around 20% of the total π^- production. In $\bar{\nu}_l$ induced π^0 production, the contribution of π^0 from the hyperon excitation is larger up to an antineutrino energy of 650 MeV than the contribution of π^0 from the Δ excitation. At $E_{\bar{\nu}} = 1$ GeV, the contribution of π^0 from the hyperon excitation is around 30% of the total π^0 production. For a more detailed discussion, please see Ref. [773, 774, 775].

https://doi.org/10.1017/9781108489065.016 Published online by Cambridge University Press

15.6.1 Inelastic production of kaons

The inelastic production of kaons from free nucleon has been discussed in Chapter 12. These amplitudes were used to study the coherent production of kaons and antikaons from nuclei [776] which has been recently observed by the MINERvA collaboration [777]. It was found that in the theoretical calculations, the cross section for coherent (anti)kaon production is considerably smaller than the pion production apart from the $\tan^2\theta_C$ suppression which arises due to the reduction in the values of nuclear form factor $F(k_\pi - q)$. Since the coherent production of particles is generally forward peaked, i.e. low q^2, most of the momentum is transferred to the nuclear system. Since the (anti)kaons have higher mass, their production needs higher (anti)neutrino energies. Thus, the momentum transfer to the nucleus is also relatively higher than the momentum transfer in case of pions. The higher value of momentum transfer to the nucleus makes the nuclear form factor quite small leading to smaller cross sections.

15.6.2 Inelastic production of photons

Other inelastic reactions studied recently include the photon emission induced by neutral currents (NC) on nucleons and nuclei and its implications in the case of quasielastic $e^{\mp}$ production in the context of neutrino oscillation experiments, for example the reactions

$$\nu(\bar{\nu}) + N \rightarrow \nu(\bar{\nu}) + N + \gamma \quad \text{(on nucleon)} \tag{15.63}$$

$$\nu(\bar{\nu}) + (A,Z) \rightarrow \nu(\bar{\nu}) + (A,Z) + \gamma \quad \text{(incoherent)} \tag{15.64}$$

$$\nu(\bar{\nu}) + (A,Z) \rightarrow \nu(\bar{\nu}) + (A,Z)_{g.s.} + \gamma \quad \text{(coherent)} \tag{15.65}$$

and shown in Figure 15.13. The first calculation of these processes at very high energies were done by Gershtein et al. [778] and Rein and Sehgal [779]. Recently, new interest in studying these reactions was awakened due to anomalous results in the quasielastic e^- production in the MiniBooNE experiment where the experimentally observed e^- yield is higher than the theoretical prediction. It has been suggested that this higher yield may be due to additional photons which are produced in these reactions; these photons decay through pair production and add to the electron yield. In this context many calculations have been done using various

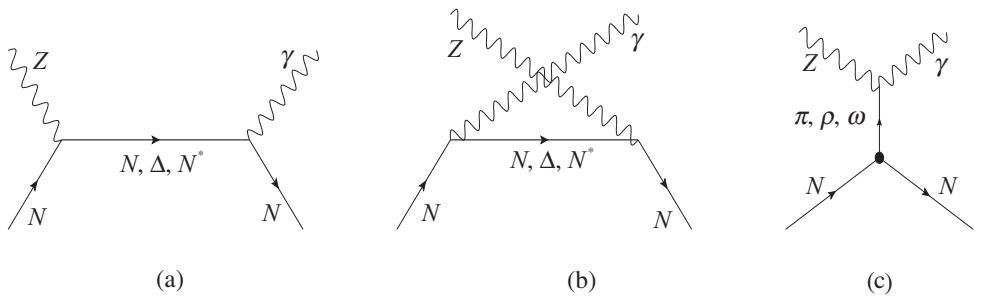

Figure 15.13 Feynman diagrams for NC photon emission. The first two diagrams are direct and crossed baryon pole terms with nucleons and resonances in the intermediate state (N,$\Delta(1232)$, N$^*(1440)$, N$^*(1520)$, etc.) The third diagram represents t channel meson (π, ρ, ω) exchange contributions.

https://doi.org/10.1017/9781108489065.016 Published online by Cambridge University Press

models and they are applied to incoherent and coherent production of photons from nuclei for the photon production using effective Lagrangians [780]. This topic has been recently reviewed by Alvarez-Ruso et al. [356].

It has been found that the photon emission by $\Delta(1232)$ and $N^*(1520)$ excited by (anti) neutrinos make the dominant contribution in the basic process. Consequently, the nuclear medium effects are very important due to the renormalization of Δ in nuclei as it is the case of the pion production. When the effect due to the Pauli blocking and Fermi motion are also taken into account, the cross sections are reduced by a factor of 30% in the region of 500 MeV to 1.5 GeV. The reduction does not depend very strongly upon the mass number A and decreases very slightly with increase in A. The incoherent cross sections are larger than the coherent cross sections. However, in the forward direction $q^2 \approx 0$, the coherent cross sections are comparable to the incoherent cross section albeit small. The theoretical calculations in various models for ^{12}C agree with each other but are not sufficient to explain the excess $e^{\pm}$ events in the MiniBooNE experiment [781]. The high energy neutrino experiment NOMAD has also searched for the neutral current (NC) single photon production at $E_\nu \approx 25$ GeV and presented a limit for this process [782]:

$$\frac{\sigma(\text{single photon})}{\sigma(\nu_\mu A \to \mu^- X)} < 4 \times 10^{-4} \;\; 90\% \; (C.L.). \tag{15.66}$$

The theoretically predicted cross sections are consistent with this limit in the relevant kinematic region.

https://doi.org/10.1017/9781108489065.016 Published online by Cambridge University Press